Electrolysis-Assisted Mn(II)/Sulfite Process for Organic Contaminant Degradation at Near-Neutral pH

Lixin Jia [1], Xingwang Pei [2,*] and Fei Yang [3]

[1]   College of Sports, Xi'an University of Architecture and Technology, Xi'an 710055, China
[2]   College of Civil Engineering, Xi'an University of Architecture & Technology, Xi'an 710055, China
[3]   College of Civil, Environmental and Geodetic Engineering, The Ohio State University, Columbus, OH 43210, USA
[*]   Correspondence: yang.2904@osu.edu

Abstract: Manganese-catalyzed sulfite activation (i.e., Mn(II)/sulfite) has emerged as an advanced oxidation process to produce sulfate radical ($SO_4^{\bullet-}$) for water treatment. However, to maintain the catalytic activity of Mn(II) ion, solution acidity has to be kept below pH 4, which is difficult to maintain in practice. Moreover, Mn(II)/sulfite reaction is a strongly oxygen-dependent process, and purging air into reaction solution is another extra cost. To solve the above issues, we devised to implement electrolysis into Mn(II)/sulfite (i.e., electro/Mn(II)/sulfite process) for organic compound (bisphenol A, BPA) oxidation. It was revealed that, under near-neutral conditions (pH 6), the removal rate of 10 μM BPA was increased from 46.3%, by Mn(II)/sulfite process, to 94.2% by electro/Mn(II)/sulfite process. The enhancement of BPA removal after implementation of electrolysis to Mn(II)/sulfite process was investigated, and concluded to be a result of several pathways. In detail, the produced oxygen from water electrolysis, direct sulfite oxidation on anode, and local acidic pH at anode vicinity together play a role in promoting $SO_4^{\bullet-}$ production and, therefore, contaminant removal. Radical-scavenging assays confirmed the dominant role of $SO_4^{\bullet-}$ in electro/Mn(II)/sulfite process.

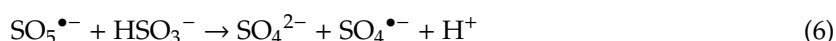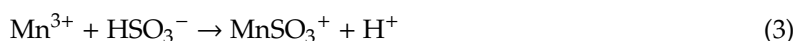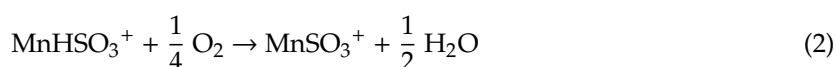**Keywords:** sulfite; advanced oxidation process; water treatment; electrolysis; electron transfer

1. Introduction

Water contamination has been a severe and widespread concern around the world, and effective and economical treatments are necessary. Advanced oxidation processes (AOPs) have been widely utilized for organic compound degradation based on oxidizing radicals such as hydroxyl radical ($HO^{\bullet}$, E = 2.73 V, NHE) [1–4]. Recently, an emerging radical, the sulfate radical ($SO_4^{\bullet-}$), has been extensively adopted for water treatment [5–7]. $SO_4^{\bullet-}$ exhibits strong oxidizing potential, as strong as $HO^{\bullet}$ [6]. $SO_4^{\bullet-}$ has been used to treat recalcitrant dyes, personal persistent organic pollutants (PPOPs), arsenic, and bacteria and viruses; moreover, $SO_4^{\bullet-}$ can be used to treat various waterbodies, including wastewater and leachate from industry, etc. [5,8–10]. The versatile application of $SO_4^{\bullet-}$ into water treatment practice has attracted great attention.

Hitherto, several processes have been used to produce $SO_4^{\bullet-}$ to support water treatment. Previously, generation of $SO_4^{\bullet-}$ has been heavily dependent on persulfate (PS) or peroxymonosulfate (PMS) under activation by heat, photolysis, photocatalysis, transition metal catalysis, and heterogeneous catalysis [5,11–13]. This method is flawed in that PS and PMS possess high stability in the environment, and the toxic undecomposed residues may affect human health upon exposure, such as through drinking water. Specifically, the LD50 (i.e., median lethal dose) for PS and PMS is reported to be 802 mg/kg [14] and 2000 mg/kg [15] by rat oral intake, respectively. Besides, PS/PMS could stably

exist in environmental media for tens of days [16–20], which further contributes to the toxicity issue to human health. To address this issue, Chen and colleagues have alternatively relied on sulfite as a $SO_4^{\bullet-}$ precursor under transition metal catalysis [21–24]. $SO_4^{\bullet-}$ could be proliferated through a series of radical chain reactions (Equations (1)–(7)) with high efficiency. Compared with PS/PMS-based processes, metal/sulfite process has the advantages of low operating cost and negligible toxicity. For instance, the LD50 for sulfite is 3560 mg/kg by rat oral intake [25], indicating a much weaker acute toxicity than PS/PMS. Moreover, sulfite is vulnerable to trace transition metal catalysis [26–28]. Researchers also showed that micromolar-level manganese ions in the aqueous phase of atmosphere could sufficiently catalyze the complete conversion of sulfite into non-toxic sulfate ion within a few minutes [29]. Real environmental media contain abundant manganese or other catalytically active transition metal ions (Cu, Cr, Fe, Co, Ni, etc.), which could catalyze sulfite oxidation. In addition, it has also been reported that, although solid sulfite is quite stable, dissolved sulfite in the aqueous solution could be oxidized simply by dissolved oxygen rapidly [30,31]. Based on the above information, it is reasoned that the use of sulfite as $SO_4^{\bullet-}$ precursor is safer than PS/PMS for water treatment purposes. Compared with other transition metal catalysts (such as Cu(II) and Co(II)) [22], iron (Fe(II)) and manganese (Mn(II)) ions have minimal cytotoxicity concern and are abundant in environmental media. In addition, Mn(II)/sulfite possesses higher oxidation potential than Fe(II)/sulfite process, especially in strongly acidic pH [22]. Therefore, in this study, Mn(II)/sulfite process was used for organic compound oxidation. The Mn(II)/sulfite process relies on the Mn(II)/Mn(III) cycle to catalyze $SO_4^{\bullet-}$ production (Equations (1)–(7)), requiring minimal Mn(II) dose in solution as a catalyst [22,24]. Moreover, it should be noted that, besides $SO_4^{\bullet-}$, Mn(II)/sulfite reaction also generates Mn(III), a strongly oxidative species that has been recently reported to rapidly oxidize a variety of organic compounds [32–34].

$$Mn^{2+} + HSO_3^- \rightarrow MnHSO_3^+ \tag{1}$$

$$MnHSO_3^+ + \frac{1}{4} O_2 \rightarrow MnSO_3^+ + \frac{1}{2} H_2O \tag{2}$$

$$Mn^{3+} + HSO_3^- \rightarrow MnSO_3^+ + H^+ \tag{3}$$

$$MnSO_3^+ \rightarrow Mn^{2+} + SO_3^{\bullet-} \tag{4}$$

$$SO_3^{\bullet-} + O_2 \rightarrow SO_5^{\bullet-} \tag{5}$$

$$SO_5^{\bullet-} + HSO_3^- \rightarrow SO_4^{2-} + SO_4^{\bullet-} + H^+ \tag{6}$$

$$HSO_3^- + SO_4^{\bullet-} \rightarrow SO_4^{2-} + H^+ + SO_3^{\bullet-} \tag{7}$$

However, in practice, the use of the Mn(II)/sulfite process faces two major concerns, which are the rapid consumption of dissolved oxygen in the solution, and the dependence of the acid to maintain Mn(II) ion catalytic activity. The above concerns were previously addressed by pumping pure oxygen or air into the solution, and adding acid to maintain optimum pH (~pH 4) [21]. These operations increase the overall operating cost and, moreover, the strong acidity is hazardous to local ecology. It is well documented that electrochemical water splitting could provide oxygen for oxygen-demanding chemical reactions, and electrodes could also regulate solution pH based on released protons or hydroxyl ions. For instance, the oxygen produced by anode has been used to support microbial degradation of vinyl chloride [35], and the local acidity created by anode was employed to catalyze hydrogen peroxide synthesis [36]. Moreover, electrolysis has been demonstrated to significantly increase the oxidation capability of Fe(II)/sulfite process for the removal of nonsteroidal anti-inflammatory drug [37], but its role in Mn(II)/sulfite process has not been examined.

In this work, we applied electrochemical water splitting into Mn(II)/sulfite process (that is, electro/Mn(II)/sulfite process), in order to address the abovementioned issues. To this end, an anode and a cathode were installed into the reaction beaker to provide oxygen and regulate local acidity around electrodes to improve Mn(II)/sulfite reaction efficiency. Bisphenol A (BPA) was chosen

as a target environmental contaminant, as BPA is an endocrine disruptor and has been widely detected in environmental media [38,39]. The BPA removal efficiency, effect of sulfite dose and current intensity, and reaction mechanism by electro/Mn(II)/sulfite process were further explored in this study. In particular, the role of Mn(III) and $SO_4^{\bullet-}$ in organics oxidation was explored in Mn(II)/sulfite and electro/Mn(II)/sulfite processes under various experimental conditions. It is anticipated that the developed electro/Mn(II)/sulfite process could address the concerns regarding the conventional Mn(II)/sulfite process, and be used as a versatile water treatment platform in future.

2. Materials and Methods

2.1. Materials

Manganese sulfate ($MnSO_4$), sodium sulfite (Na_2SO_3), bisphenol A (BPA, $C_{15}H_{16}O_2$), and sodium sulfate (Na_2SO_4) were purchased from Sigma-Aldrich Co., Ltd. (Shanghai, China). Ethanol and *tert*-butanol, used as radical scavengers of $SO_4^{\bullet-}$ and $HO^\bullet$, were from Fisher Scientific Ltd. (Hampton, NH, USA). Other chemicals, including rhodamine B, congo red, orange II, methyl orange, atrazine, metoprolol, phenol, 4-chlorophenol, amoxicillin, phosphoric acid, methanol, and acetonitrile were obtained from Fisher Scientific Ltd. (Hampton, NH, USA). These chemicals were used as degradation substrates and mobile phase for analysis, respectively. Two mixed metal oxide (MMO) mesh electrodes (2 cm × 6 cm) (Xi'an Ocean Material Technology Co., Ltd., Xi'an, China) were used in this study. MMO electrodes are relatively stable and have been tested in groundwater conditions. Previous reports indicated that MMO electrodes could be used in groundwater for years without any poisoning by organics or inorganic ions [36].

2.2. Batch Reaction of BPA Removal

The reactor configuration is described in Figure 1. In a typical assay, 0.2 mM $MnSO_4$, 2 mM sulfite, 5 mM sulfate as supporting electrolyte, and 10 μM BPA were prepared in the 200 mL reaction solution. Solution pH was rapidly adjusted to pH 6 with diluted NaOH and H_2SO_4. The reaction was initiated by turning on the power supply (Agilent E3617A model) that was connected to the MMO electrodes. The electric current was set constant at 100 mA. In other assays, the sulfite concentration and electric current applied into the reaction solution were changed as indicated. At specific time intervals, 1 mL reaction solution was sampled and filtered using a 0.45 μm membrane (Millipore, Burlington, MA, USA) to remove manganese hydroxide precipitate particles. The reaction solution sample was then loaded onto high-performance liquid chromatography (HPLC, Agilent 1200 series) for analysis. BPA was separated by using methanol/water 60:40 as the mobile phase, and Agilent ZORBAX Eclipse Plus C18 (4.6 × 100 mm 5 μm) as the column. The detection wavelength was 230 nm. In Section 3.5, other contaminants were also used as substrates of electro/Mn(II)/sulfite process, and the analysis method was included.
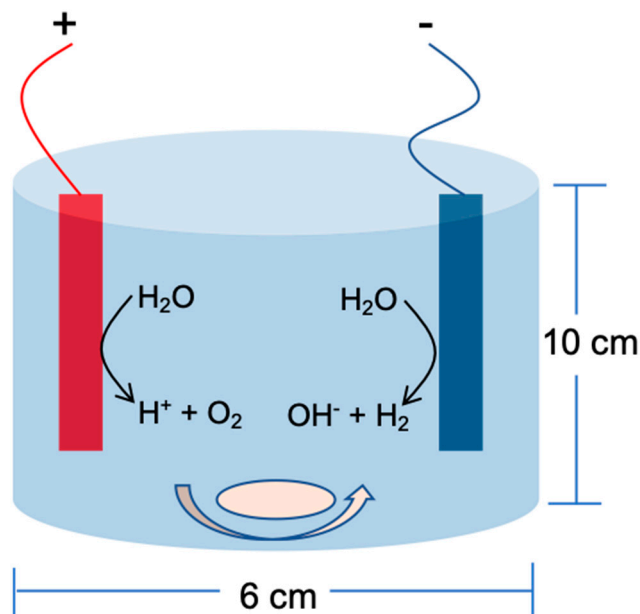
Figure 1. Configuration of the reactor for electro/Mn(II)/sulfite process. Reactor dimension was included, and reaction was under constant stirring. "+" and "−" denotes anode and cathode, respectively.

2.3. BPA Removal by Electro/Mn(II)/Sulfite Process in Divided Electrochemical Cell

Two separate beakers (divided cells, 150 mL volume of each reactor) were connected by a channel with a Nafion selective membrane in the middle, and anode was inserted into one chamber while cathode was inserted into the other chamber. In each chamber, 100 mL (pH 6) of 0.2 mM $MnSO_4$, 2 mM sulfite, 5 mM sulfate as supporting electrolyte, and 10 µM BPA were added into each chamber. Solutions were under constant magnetic stirring. Reactions were initiated by switching on power supply (Agilent E3617A model) to maintain a constant electric current at 100 mA, and BPA concentration, solution pH, and dissolved oxygen content in each chamber were monitored.

2.4. Measurement of MnO_2 Concentration

MnO_2 concentration was measured based on a previous report [40]. In detail, 1 mL sampled solution was added into 1 mL 200 µM 2,2'-azino-bis(3-ethylbenzothiazoline-6-sulfonate) (ABTS) in 20 mM HEPES buffer (pH 6), and a green $ABTS^{\bullet+}$ product developed within 5 min. The samples were measured with a UV–Vis spectrometer at 645 nm. 0–200 µM MnO_2 was used as standard solutions for calibration purpose.

2.5. Measurement of Formaldehyde Concentration

Methanol (10 mM) was added into Mn(II)/sulfite or electro/Mn(II)/sulfite processes at indicated conditions. The produced formaldehyde in 1 mL sample was first derivatized by adding 0.5 mL 500 µM 2,4-dinitrophenylhydrazine (DNPH). The formed formaldehyde–DNPH adduct has a strong absorption at 360 nm and was detected by HPLC. The formaldehyde–DNPH product was separated by water/acetonitrile (55:45 (v/v)) mobile phase at a flow rate of 1 mL/min. This method has a detection limit of 0.1 ppm [41].

2.6. Radical-Scavenging Assay
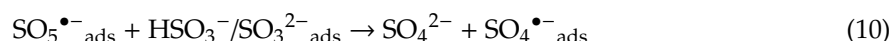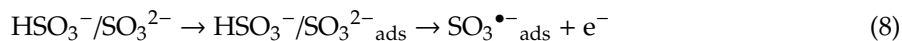
In order to study the role of $SO_4^{\bullet-}$ in BPA degradation, selective radical scavengers were added into the reaction solution. In detail, ethanol (strong $SO_4^{\bullet-}$ scavenger) and *tert*-butanol (inert to $SO_4^{\bullet-}$) were prepared into the electro/Mn(II)/sulfite reaction solution at indicated concentrations (5 or 10 mM), while other parameters were fixed (i.e., 0.2 mM $MnSO_4$, 2 mM sulfite, 5 mM sulfate as supporting

electrolyte, 10 μM BPA, 100 mA electric current, and pH 6). The BPA removal rate was monitored at specific time interval by taking samples and analysis with HPLC as stated in Section 2.2 (i.e., methanol/water 60:40 as the mobile phase, detection wavelength was 230 nm).

3. Results and Discussion

3.1. Removal of BPA by Electro/Mn(II)/Sulfite Process

BPA removal results by electro/Mn(II)/sulfite process and related controls are shown in Figure 2. Negligible BPA removal was observed after individual treatment by electricity, Mn(II), and sulfite solution, indicating that BPA was insensitive to electrode electrolysis. Electro/Mn(II) reaction did not mediate any BPA removal, suggesting that no reactive species, such as Mn(III), were generated on electrodes. At pH 6, Mn(II)/sulfite reaction showed weak oxidation capacity, and removed 46.3% of 10 μM BPA. Electro/sulfite reaction also produced slight BPA removal, consistent with previous report [37]. This is because sulfite could be oxidized on anodes, through direct electron transfer procedure [37,42]. The produced $SO_3^{\bullet-}$ then evolved into $SO_4^{\bullet-}$ by oxygen, that could oxidize organic compounds in the solution (Equations (8)–(10)). In order to further study reactions on anode, the applied potential was measured. Results indicated that applied potential to the anode was measured to be 1.4–1.5 V (vs. SHE). The redox potential of H_2O/O_2 is 1.23 V (vs. SHE), Mn(II/III) is 1.51 V (vs. SHE) [43], and SO_3^{2-}/SO_3^- is 0.63–0.84 V (vs. SHE) [27,44]. Hence, within the applied potential range, water and sulfite could be oxidized, while Mn(II) oxidation into Mn(III) and sulfate ion oxidation into $SO_4^{\bullet-}$ on the anode is highly improbable considering essential overpotential and reaction rate to support sufficient production of reactive species. Results indicated that electro/Mn(II)/sulfite process removed 94.2% of 10 μM BPA within 40 min, significantly higher than the above controls. The role of electrolysis needs more investigation.

$$HSO_3^-/SO_3^{2-} \rightarrow HSO_3^-/SO_3{}^{2-}{}_{ads} \rightarrow SO_3^{\bullet-}{}_{ads} + e^- \tag{8}$$

$$SO_3^{\bullet-}{}_{ads} + O_2 \rightarrow SO_5^{\bullet-}{}_{ads} \tag{9}$$

$$SO_5^{\bullet-}{}_{ads} + HSO_3^-/SO_3{}^{2-}{}_{ads} \rightarrow SO_4^{2-} + SO_4^{\bullet-}{}_{ads} \tag{10}$$

To discern the role of electrolysis in the Mn(II)/sulfite process, dissolved oxygen content and solution pH were monitored. As shown in Figure 2b, in conventional Mn(II)/sulfite process, the dissolved oxygen content rapidly decreased to 3.59 mg/L although this reaction is slow at pH 6. At pH 4, which is the optimum solution acidity for the Mn(II)/sulfite process, the complete depletion of dissolved oxygen can be achieved within a few seconds [24]. The consumption of dissolved oxygen is due to Equations (2) and (5), the latter of which plays an especially significant role. A previous investigation has shown that, by purging nitrogen in the metal/sulfite reaction solution, the decolorization of an organic dye compound can be fully stalled [21]. This indicates that oxygen is necessary to produce $SO_4^{\bullet-}$ radical by the Mn(II)/sulfite process. In the electro/Mn(II)/sulfite process, however, the solution dissolved oxygen content was maintained at around 8.19 mg/L during the first 5 min, and then slightly increased to 8.79 mg/L at the end of reaction (Figure 2b). The high oxygen concentration by electrolysis led to more $SO_4^{\bullet-}$ radical production, which mediated a higher BPA removal efficiency.

Figure 2c shows the solution pH change during Mn(II)/sulfite and electro/Mn(II)/sulfite processes. In the Mn(II)/sulfite process, the solution pH gradually decreased, and it reached pH 5.67 at 10 min, and pH 4.89 at the end of reaction. The decrease of solution pH is due to sulfite being a Lewis base, and its oxidation could lead to solution acidification. The pH decrease by Mn(II)/sulfite process with an original pH 6 was slow because of the retarded catalytic transformation of sulfite under near-neutral pH. In electro/Mn(II)/sulfite process, however, remarkable solution acidification was observed. The significant pH decrease started at 5 min, and reached pH 3.12 at 40 min. Two pathways could account for the intensive pH acidification by electro/Mn(II)/sulfite process. At first, as shown above, the oxygen produced by anode could accelerate the overall Mn(II)/sulfite reaction, which then

acidified solution pH via consuming sulfite. Second, the anode vicinity exhibits a strong acidity (measured as pH 3.8 during our study, data not shown). This acidity around the anode is especially favored by Mn(II)/sulfite reaction, which then, in turn, also led to solution acidification. Consequently, it is recognized, overall, that both produced oxygen and local acidity around the anode contributed to the enhanced BPA removal by the electro/Mn(II)/sulfite process [37].
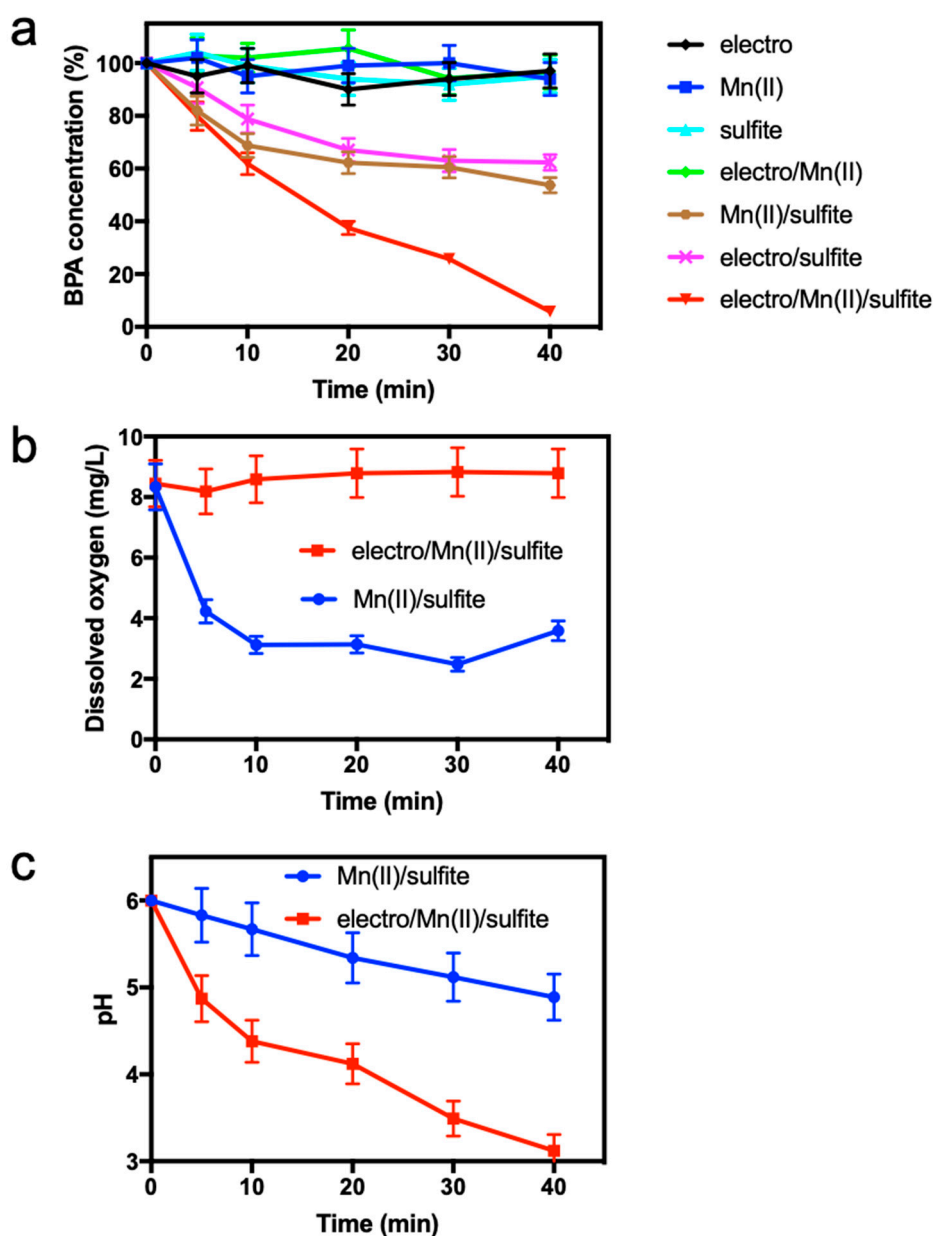

Figure 2. Removal of bisphenol A (BPA) by the electro/Mn(II)/sulfite process. (**a**) BPA removal by several controls; (**b**) dissolved oxygen in the solution changes in Mn(II)/sulfite and electro/Mn(II)/sulfite processes; and (**c**) solution pH changes in Mn(II)/sulfite and electro/Mn(II)/sulfite processes. Reaction conditions: 0.2 mM Mn(II), 2 mM sulfite, 5 mM sulfate as supporting electrolyte, 10 μM BPA, 100 mA electric current, and pH 6.

In order to further study the role of electrolysis in electro/Mn(II)/sulfite process, the assay was performed in a divided electrochemical cell with a Nafion selective membrane that only allows protons to cross. BPA degradation by Mn(II)/sulfite process was monitored in both anode and cathode chambers (Figure 3a). As shown, 45.7% of BPA was removed in the cathode chamber over the course of reaction.

However, in the anode chamber, BPA was rapidly degraded, and 66.9% of 10 μM BPA was removed within 10 min. The BPA removal by Mn(II)/sulfite process in the anode chamber was faster than undivided electro/Mn(II)/sulfite process. The measurements of dissolved oxygen content (Figure 3b) and solution pH (Figure 3c) confirmed that the anode chamber produced oxygen and acidic pH that are favored by Mn(II)/sulfite reaction.
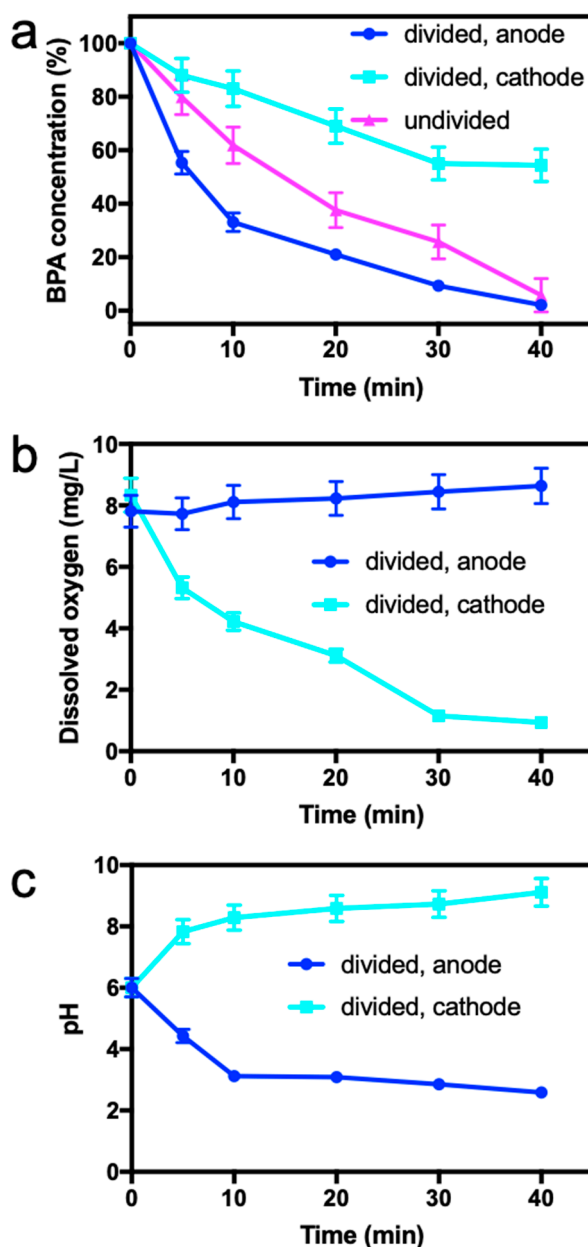

Figure 3. Removal of BPA by the electro/Mn(II)/sulfite process in divided electrochemical cell. (**a**) BPA removal by the electro/Mn(II)/sulfite process in anode and cathode chambers and undivided electrochemical cell; (**b**) dissolved oxygen in the solution changes in anode and cathode chambers; and (**c**) solution pH changes in anode and cathode chambers. Reaction conditions: 0.2 mM Mn(II), 2 mM sulfite, 5 mM sulfate as supporting electrolyte, 10 μM BPA, 100 mA electric current, and pH 6.

3.2. Effect of Sulfite Dose

Sulfite is the precursor of $SO_4^{\bullet-}$, and it has a complex role in $SO_4^{\bullet-}$ radical generation. Specifically, as reported previously, low sulfite dose is proportional to $SO_4^{\bullet-}$ radical yield, whereas high sulfite dose could retard $SO_4^{\bullet-}$ radical generation through self-scavenging (Equation (7)). This is because

overdosed sulfite could compete with organic substrates to consume $SO_4^{\bullet-}$, leading to lower substrate removals. To figure out the role of sulfite dose in the electro/Mn(II)/sulfite process, sulfite concentrations of 0–4 mM were used, with other parameters fixed, and the BPA removal results are shown in Figure 4.
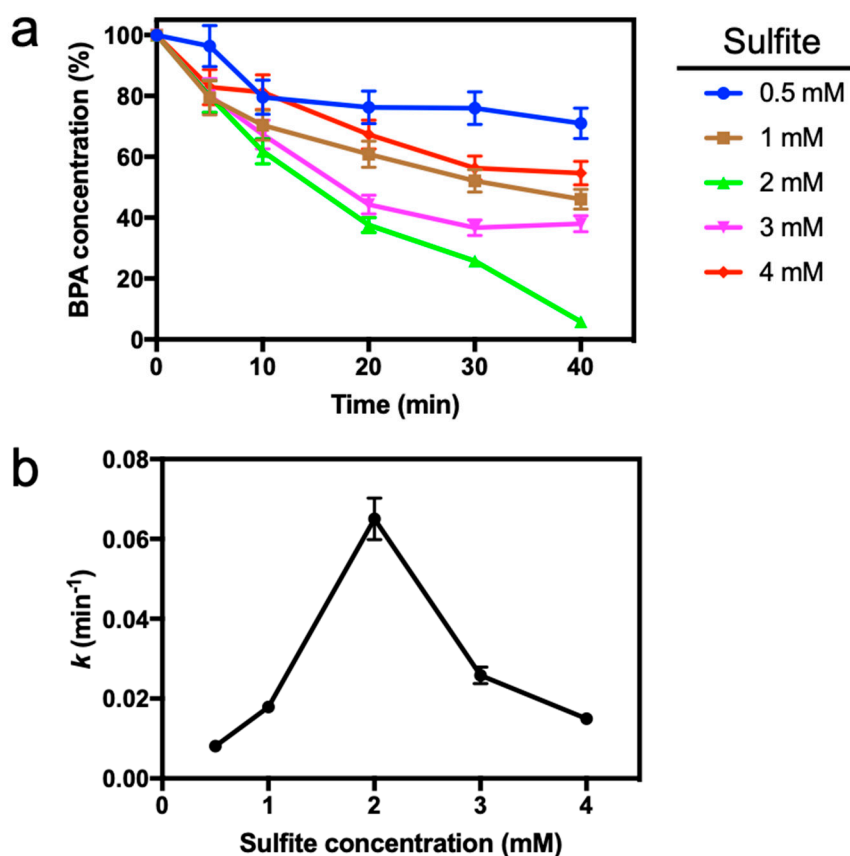

Figure 4. Effect of sulfite dose on the BPA removal by the electro/Mn(II)/sulfite process. (**a**) BPA removal and (**b**) pseudo first-order removal constant versus sulfite concentration. Reaction conditions: 0.2 mM Mn(II), 0.5–4 mM sulfite, 5 mM sulfate as supporting electrolyte, 10 μM BPA, 100 mA electric current, and pH 6.

As observed, the BPA removal improved with increasing sulfite concentration when sulfite was below 2 mM. For instance, the eventual BPA removal at 0.5, 1, and 2 mM sulfite was 29%, 53.9%, and 94.2%, respectively. However, as sulfite concentration was further increased to over 2 mM, BPA removal was weakened. The BPA removal at 4 mM sulfite was 45.3% at the end of reaction. The pseudo first-order kinetics were used to fit BPA removal curves (Figure 4b). As shown, the pseudo first-order reaction constant of BPA removal (k) by electro/Mn(II)/sulfite process at 0.5, 1, 2, 3, and 4 mM sulfite was 0.0081, 0.0179, 0.065, 0.0258, and 0.015 min^{-1}, respectively. The effect of sulfite concentration was consistent with previous reports [21–24].

3.3. Effect of Current Intensity

The role of electric current was explored in the range of 0–200 mA for BPA removal by electro/Mn(II)/sulfite process. As shown in Figure 5a, as the electric current increased, the BPA removal rate was also improved. For instance, the BPA removal rate at 20, 50, and 100 mA current was 58.6%, 72%, and 94.2%, respectively. The BPA removal curves were also re-plotted using pseudo first-order kinetics, and results are shown in Figure 5b. It was observed that the increase of the pseudo first-order removal constant of BPA (k) was remarkable in the range of 0–100 mA electric current. However, beyond the range of 100 mA current intensity, the increase of k became negligible.
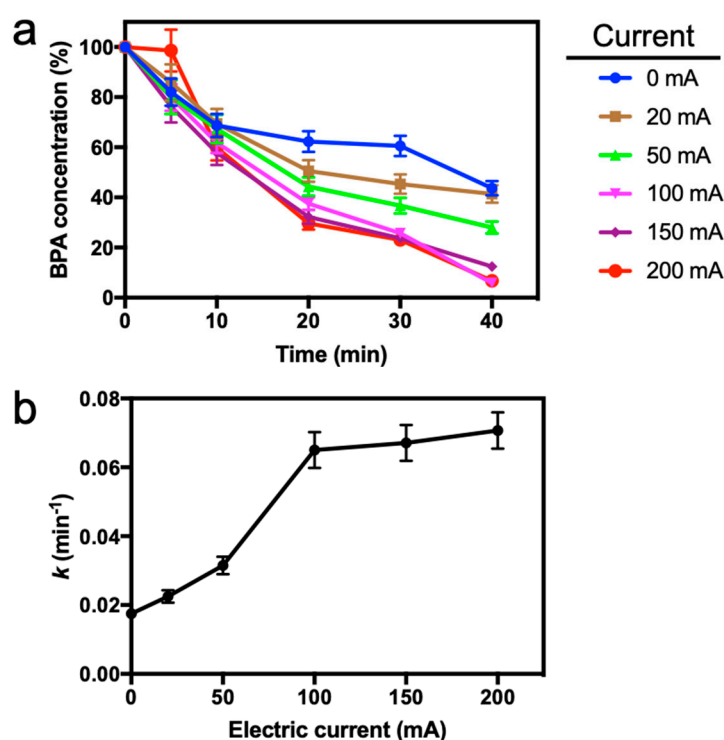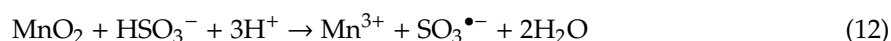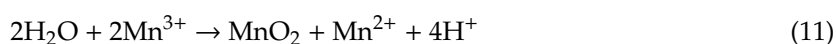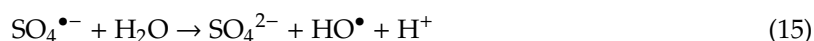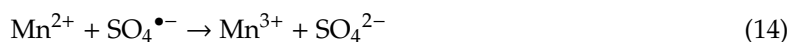
Figure 5. Effect of electric current on the BPA removal by the electro/Mn(II)/sulfite process. (**a**) BPA removal and (**b**) pseudo first-order removal constant versus electric current. Reaction conditions: 0.2 mM Mn(II), 2 mM sulfite, 5 mM sulfate as supporting electrolyte, 10 μM BPA, 0–200 mA electric current, and pH 6.

As mentioned above, several pathways might account for the role of electricity in the electro/Mn(II)/sulfite process. First, the oxygen produced by the anode could drive more $SO_4^{\bullet-}$ generation and, second, sulfite could be directly oxidized by the anode into $SO_3^{\bullet-}$ which also eventually evolves into $SO_4^{\bullet-}$. Higher electric current leads to enhanced effects in both of the above pathways, which accounted for the positive correlation between electric current and BPA removal in the range of 0–100 mA. However, as the electric current further increased to above 100 mA, the dissolved oxygen in the solution was saturated, and the sparked $SO_3^{\bullet-}$ by anode oxidation reached a plateau as its production was limited to the adsorbed amount of SO_3^{2-} molecules [37]. As a result, the further increase of BPA removal at above 100 mA electric current was not significant.

3.4. Mechanism Study

As shown in Equations (1)–(7), a mixture of oxysulfur radicals ($SO_3^{\bullet-}$, $SO_5^{\bullet-}$, and $SO_4^{\bullet-}$) could be produced by the electro/Mn(II)/sulfite process. These oxysulfur radicals have exhibited distinct properties in reaction with organic compounds. In a previous report, it has been summarized that $SO_3^{\bullet-}$ has weak reduction capability, $SO_5^{\bullet-}$ can selectively oxidize amines, while $SO_4^{\bullet-}$ possesses much broader selectivity toward a wide range of organic compounds and possibly plays the most significant role in BPA removal in this study [23,37]. Moreover, it is worth noting that Mn(III), a strongly oxidative species, was reported to be generated in Mn(II)/sulfite reaction (Equations (2), (3) and (12)). The presence of Mn(III) has been previously confirmed via pyrophosphate, and Mn(III) is able to rapidly remove organic compounds in tens of seconds [32–34]. The disproportion of Mn(III) could also generate Mn(IV) (Equation (11)).

$$2H_2O + 2Mn^{3+} \rightarrow MnO_2 + Mn^{2+} + 4H^+ \tag{11}$$

$$MnO_2 + HSO_3^- + 3H^+ \rightarrow Mn^{3+} + SO_3^{\bullet-} + 2H_2O \tag{12}$$

$$Mn^{3+} + OC \rightarrow Mn^{2+} + OC^{\bullet+} \text{ (OC, organic compound)} \tag{13}$$

$$Mn^{2+} + SO_4^{\bullet-} \rightarrow Mn^{3+} + SO_4^{2-} \tag{14}$$

$$SO_4^{\bullet-} + H_2O \rightarrow SO_4^{2-} + HO^{\bullet} + H^+ \tag{15}$$

$$SO_4^{\bullet-} + HO^- \rightarrow SO_4^{2-} + HO^{\bullet} \tag{16}$$

In order to discern the role of reactive species, a radical-scavenging approach was adopted. In detail, we individually added ethanol and *tert*-butanol into the electro/Mn(II)/sulfite-treated BPA solution. Ethanol could react with $SO_4^{\bullet-}$ with relatively high activity [45], while *tert*-butanol is inert toward $SO_4^{\bullet-}$ [46]. Besides, ethanol and *tert*-butanol are reported to be both inert to Mn(III), as Mn(III) is an electrophilic oxidant [34]. This method has been widely used to distinguish if $SO_4^{\bullet-}$ plays a role in certain oxidation process [47–50]. As shown in Figure 6, addition of 5 and 10 mM *tert*-butanol showed little effect in BPA removal kinetics. The slight difference between control group and the group with *tert*-butanol was due to the reaction between *tert*-butanol and $SO_4^{\bullet-}$, because although *tert*-butanol is inert to $SO_4^{\bullet-}$ (9.1×10^5 M^{-1} s^{-1}) [51], the concentration of *tert*-butanol used in this study (5 or 10 mM) was 500–1000 times higher than the used BPA concentration. By comparison, 10 mM ethanol fully inhibited BPA removal, and decreased the BPA removal kinetic constant from 0.065 to 0.0034 min^{-1}. Additionally, it has been reported that $HO^{\bullet}$ could also be produced from the reaction between $SO_4^{\bullet-}$ and water or HO^- (Equations (15) and (16)), which could oxidize a large variety of organic compounds. *tert*-Butanol (6×10^8 M^{-1} s^{-1}) and ethanol (1.9×10^9 M^{-1} s^{-1}) [52] are strong scavengers of $HO^{\bullet}$. The addition of 5 or 10 mM *tert*-butanol mediated slight decrease of BPA removal, suggesting that $HO^{\bullet}$ was not a major contributor for BPA removal. Overall, above results thus indicated that $SO_4^{\bullet-}$ was completely responsible for BPA oxidation in the electro/Mn(II)/sulfite process.
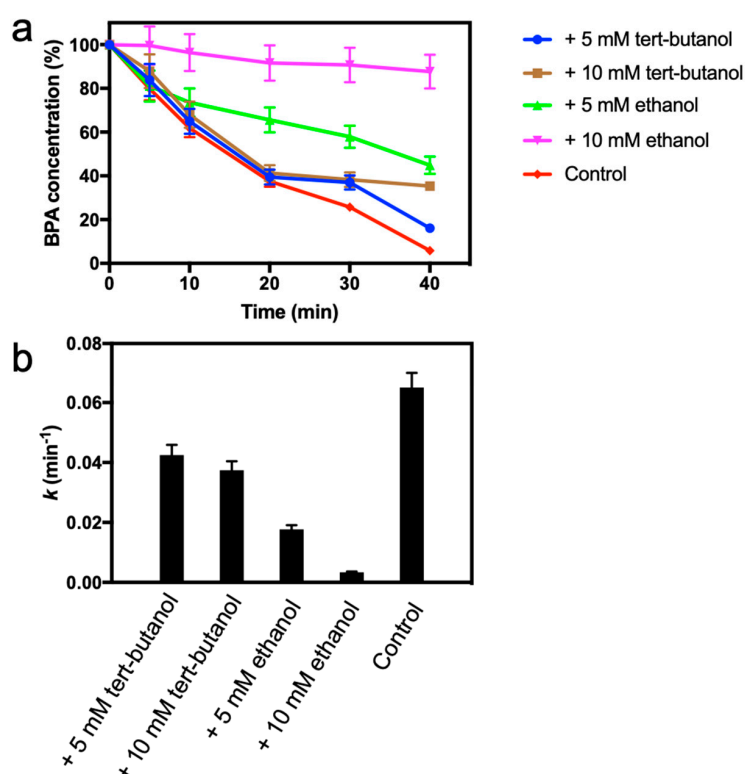

Figure 6. Radical-scavenging assay of the electro/Mn(II)/sulfite process. (**a**) BPA removal and (**b**) pseudo first-order removal constant after addition of radical scavengers. Reaction conditions: 0.2 mM Mn(II), 2 mM sulfite, 5 mM sulfate as supporting electrolyte, 10 μM BPA, 100 mA electric current, and pH 6. Ethanol and *tert*-butanol at indicated concentration was added to reaction solution. Control indicates no addition of radical scavenger.

Previous studies suggested that, under certain circumstances, both Mn(III) and $SO_4^{\bullet-}$ could be generated and play a significant role in organic compound oxidation in manganese-catalyzed sulfite activation processes, such as permanganate/sulfite, MnO_2/sulfite, and Mn(II)/sulfite reactions [32–34,40]. Studies have reported that solution pH might affect the species responsible for organic compound oxidation. For instance, MnO_2/sulfite reaction at near-neutral pH produces Mn(III) for organic compound removal [34], while Mn(II)/sulfite reaction at acidic pH generates $SO_4^{\bullet-}$ for substrate oxidation [40]. Moreover, the mutual conversion of MnO_2 and Mn(II) could be mediated by sulfite (Equations (11)–(14)). At first, the produced MnO_2 by Mn(II)/sulfite and electro/Mn(II)/sulfite processes at different solution pH was quantified (Figure 7a). It was shown that, as solution pH increased, the produced MnO_2 was improved for both Mn(II)/sulfite and electro/Mn(II)/sulfite processes. Moreover, Mn(II)/sulfite produced more MnO_2 than electro/Mn(II)/sulfite process, probably because of lower final pH in electro/Mn(II)/sulfite process (Figure 7b). The final measured solution pH of Mn(II)/sulfite and electro/Mn(II)/sulfite process with an initial pH of 6 were pH 4.89 and 3.12, respectively. Our results are consistent with a previous report [40].
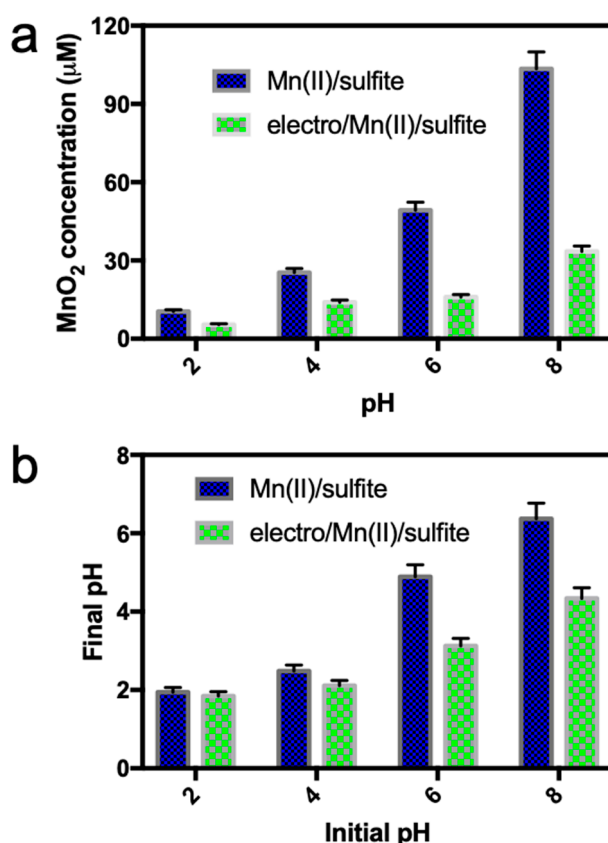

Figure 7. Quantification of produced MnO_2 (**a**) and measurement of final solution pH (**b**) in Mn(II)/sulfite and electro/Mn(II)/sulfite processes at different initial pH. Reaction conditions: 0.2 mM Mn(II), 2 mM sulfite, 5 mM sulfate as supporting electrolyte, 10 μM BPA, and 100 mA electric current. Initial solution pH varied as indicated.

The contribution of Mn(III) and $SO_4^{\bullet-}$ towards BPA oxidation was further tested with a rational semi-quantitative method. In detail, as demonstrated above, *tert*-butanol and ethanol could discern the role of $SO_4^{\bullet-}$. Besides, we tested if Mn(III) played a role by measuring its oxidation products of methanol because $SO_4^{\bullet-}$ oxidizes alcohol into formaldehyde while Mn(III) cannot [34]. BPA removal by Mn(II)/sulfite (Figure 8a) and electro/Mn(II)/sulfite (Figure 8b) process after addition of *tert*-butanol and ethanol was monitored. It is interesting to note that, in the range of pH 2–6, higher solution pH decreased BPA removal efficiency for Mn(II)/sulfite process, i.e., 95.38% at pH 2 and 56.3% at pH 6.

However, at pH 8, the BPA removal was improved up to 89.4% at the end of reaction. The role of reactive species in Mn(II)/sulfite process at pH 8 was studied. The radical-scavenging assay results indicated that $SO_4^{\bullet-}$ did not likely played a major role in BPA removal at pH 8 in Mn(II)/sulfite process. The oxidation of methanol into formaldehyde was also measured (Figure 8c). Results indicated that at pH 8, negligible formaldehyde was observed in Mn(II)/sulfite process, indicating that Mn(III) instead of $SO_4^{\bullet-}$ accounted for BPA removal. In sharp contrast, the BPA removal efficiency by electro/Mn(II)/sulfite process decreased at higher solution pH in the range of pH 2–8 (Figure 8b). Moreover, radical-scavenging assay results indicated that $SO_4^{\bullet-}$ played a major role in BPA removal regardless of solution pH (Figure 8b). Such a conclusion was further confirmed by the detection of produced formaldehyde (Figure 8c).
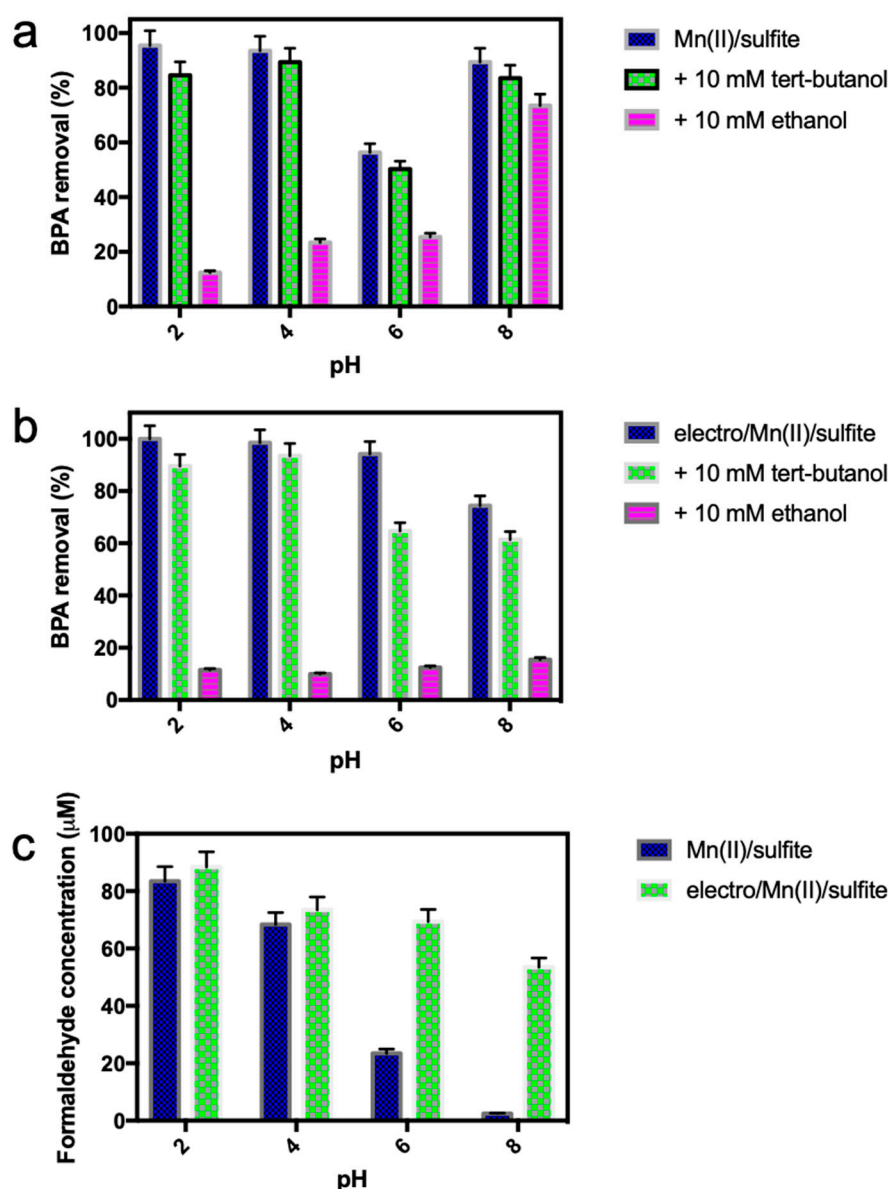

Figure 8. BPA removal by Mn(II)/sulfite (**a**) and electro/Mn(II)/sulfite (**b**) processes at different pH and addition of 10 mM *tert*-butanol or 10 mM ethanol, and produced formaldehyde by Mn(II)/sulfite and electro/Mn(II)/sulfite process at different pH (**c**). Reaction conditions: 0.2 mM Mn(II), 2 mM sulfite, 5 mM sulfate as supporting electrolyte, 10 μM BPA, and 100 mA electric current. Initial solution pH varied as indicated. (**c**) Formaldehyde was generated between $SO_4^{\bullet-}$ and 10 mM methanol.

Consequently, the following conclusions could be drawn from above results: (1) $SO_4^{\bullet-}$ played a major role in BPA removal by Mn(II)/sulfite process at pH below 6; (2) Mn(III) accounted for BPA removal by the Mn(II)/sulfite process at pH 8; and (3) $SO_4^{\bullet-}$ was completely responsible for BPA removal by the electro/Mn(II)/sulfite process, presumably because of the acidic conditions mediated by electrolysis. The reaction mechanism for electro/Mn(II)/sulfite is shown in Figure 9.
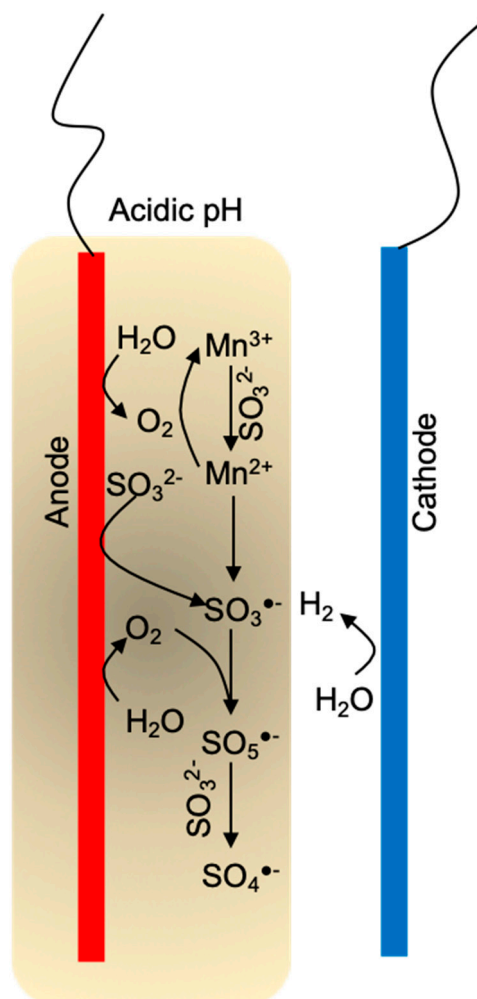

Figure 9. Schematic reaction mechanism of the electro/Mn(II)/sulfite process.

3.5. Degradation of Other Organic Pollutants

The capability of the electro/Mn(II)/sulfite process to degrade other organic pollutants was tested. Nine organic compounds were selected to represent the commonly detected pollutants in the environmental medium, and their quantification methods were included in Table 1. Among them, rhodamine B, congo red, orange II, and methyl orange are organic dyes which were analyzed by UV–Vis spectrometry. Atrazine, metoprolol, phenol, 4-chlorophenol, and amoxicillin were quantified by high-performance liquid chromatography (HPLC).

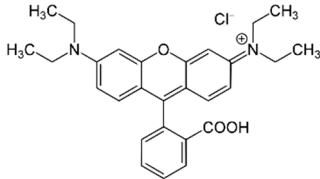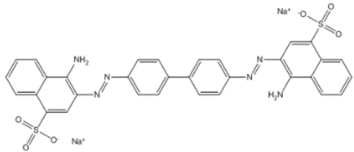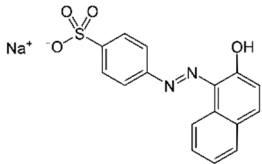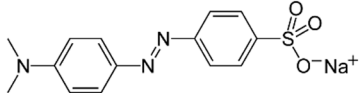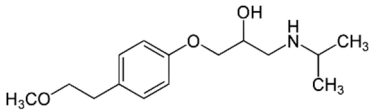**Table 1.** Quantification methods for selected organic compounds.
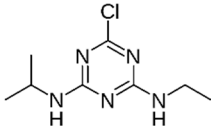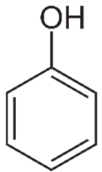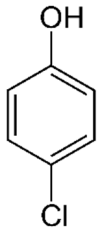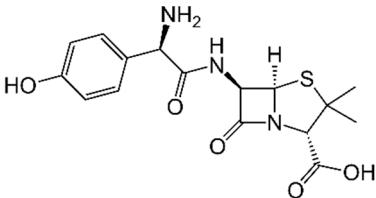
Name	Structure	Chemical Formula	Quantification Method	Mobile Phase	Detection Wavelength (nm)
Rhodamine B		$C_{28}H_{31}ClN_2O_3$	UV–Vis spectrometer	n.a.	545
Congo Red		$C_{32}H_{22}N_6Na_2O_6S_2$	UV–Vis spectrometer	n.a.	498
Orange II		$C_{16}H_{11}N_2NaO_4S$	UV–Vis spectrometer	n.a.	485
Methyl Orange		$C_{14}H_{14}N_3NaO_3S$	UV–Vis spectrometer	n.a.	464
Atrazine		$C_8H_{14}ClN_5$	HPLC	Methanol/water 60:40	230

Table 1. *Cont.*

Name	Structure	Chemical Formula	Quantification Method	Mobile Phase	Detection Wavelength (nm)
Metoprolol		$C_{15}H_{25}NO_3$	HPLC	Methanol/KH$_2$PO$_4$ (pH 3) 60:40	230
Phenol		C_6H_6O	HPLC	Methanol/water 65:35	270
4-Chlorophenol		C_6H_5ClO	HPLC	5 mmol H$_2$SO$_4$/methanol 80:20	270
Amoxicillin		$C_{16}H_{19}N_3O_5S$	HPLC	Acetonitrile/KH$_2$PO$_4$ (pH 3) 22:78	254

Results showed that removal rates of all tested organic compounds at a concentration of 10 μM by the electro/Mn(II)/sulfite process were above 85% (Figure 10). In particular, the degradation of organic dyes was, in general, more pronounced than the other compounds, possibly because the dyes possess electrophilic chromophore groups that are easily oxidized by $SO_4^{\bullet-}$. Moreover, the degradation of metoprolol (a beta-blocker to treat high blood pressure, chest pain, and heart failure) showed the lowest efficiency (85.4%) by electro/Mn(II)/sulfite process, due to the weak oxidation capacity of $SO_4^{\bullet-}$ toward electrophilic functional groups such as saturated C–C bonds. Above results demonstrated that electro/Mn(II)/sulfite process could non-selectively degrade a wide variety of organic compounds, therefore demonstrating strong potential toward practical applications.
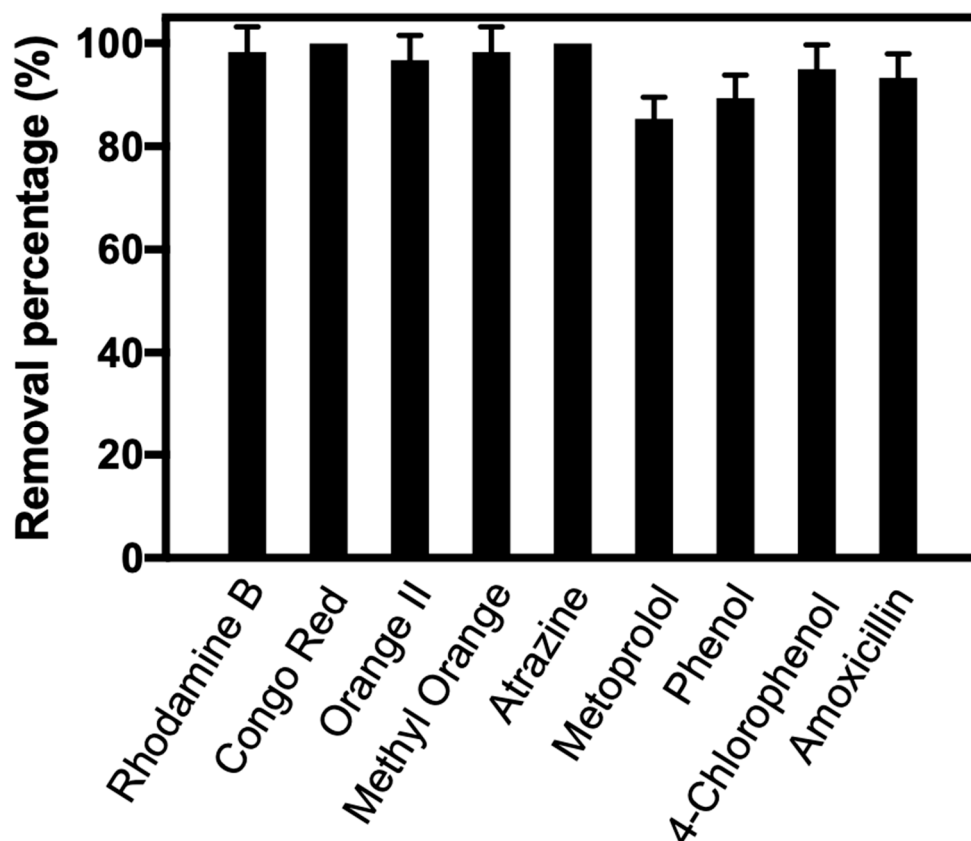

Figure 10. Degradation of selected compounds by the electro/Mn(II)/sulfite process. Reaction conditions: 0.2 mM Mn(II), 2 mM sulfite, 5 mM sulfate as supporting electrolyte, 10 μM organic compound, 100 mA electric current, and pH 6.

4. Conclusions

In this work, electrolysis was applied to Mn(II)/sulfite process, in order to realize effective water treatment in near-neutral conditions. At pH 6, the BPA removal was increased from 46.3% by Mn(II)/sulfite process to 94.2% by electro/Mn(II)/sulfite process. The synergetic role of electrolysis was investigated, and results indicated that it mainly affects two pathways of promoting $SO_4^{\bullet-}$ generation. At first, the oxygen produced by anode from water electrolysis is used to improve oxysulfur radical evolution (Equations (1)–(7)), and eventually mediates higher yield of $SO_4^{\bullet-}$ and results in higher BPA removal. Second, sulfite could be oxidized on the anode through direct electron transfer, i.e., the electron was transferred from sulfite to anode without catalyst (Equations (8)–(10)). The above mechanisms demonstrated in this study are consistent with previous studies. The contribution of Mn(III) toward BPA removal was also tested, and Mn(III) unlikely plays a significant role in BPA oxidation in electro/Mn(II)/sulfite process. However, Mn(III) was dominant in BPA oxidation in Mn(II)/sulfite process at high pH (such as above pH 6), as shown in this study. It should also be

noted that the pH profile in the solution could also be regulated in the vicinity around the electrode, and the pH in the anode vicinity was measured as pH 3.8. This local acidity could also accelerate the Mn(II)/sulfite process for BPA removal. Together, these roles of electrolysis contribute to the high oxidizing efficiency of electro/Mn(II)/sulfite process toward organic compound removal.

This study has great implications in practice. For instance, most natural waterbodies are near-neutral, at which the conventional Mn(II)/sulfite or other transition metal-based AOPs are ineffective. Our developed electro/Mn(II)/sulfite process avoids the addition of acid into the solution, thus reducing the cost. Moreover, compared with PS/PMS or hydrogen peroxide, which are often used as radical precursors for water treatment, sulfite is cheaper and more readily to produce in industrial scale. Besides, an ideal niche of this work should be the treatment of lightly polluted waterbodies where ozone oxidation or other costly processes are ineffective. For instance, the electro/Mn(II)/sulfite process could be used to treat contaminated groundwater. This is because Mn(II)-containing minerals are abundant in groundwater matrices which could release Mn(II) ions. Considering all the above, it is thus reasoned that this process holds great potential for the water treatment industry.

References

1. Wardman, P. Reduction Potentials of One-Electron Couples Involving Free Radicals in Aqueous Solution. *J. Phys. Chem. Ref. Data* **1989**, *18*, 1637–1755. [CrossRef]

2. Deng, Y.; Zhao, R. Advanced oxidation processes (AOPs) in wastewater treatment. *Curr. Pollut. Rep.* **2015**, *1*, 167–176. [CrossRef]

3. Dewil, R.; Mantzavinos, D.; Poulios, I.; Rodrigo, M.A. New perspectives for advanced oxidation processes. *J. Environ. Manag.* **2017**, *195*, 93–99. [CrossRef] [PubMed]

4. Asghar, A.; Raman, A.A.A.; Daud, W.M.A.W. Advanced oxidation processes for in-situ production of hydrogen peroxide/hydroxyl radical for textile wastewater treatment: A review. *J. Clean Prod.* **2015**, *87*, 826–838. [CrossRef]

5. Wacławek, S.; Lutze, H.V.; Grübel, K.; Padil, V.V.; Černík, M.; Dionysiou, D.D. Chemistry of persulfates in water and wastewater treatment: A review. *Chem. Eng. J.* **2017**, *330*, 44–62. [CrossRef]

6. Anipsitakis, G.P.; Dionysiou, D.D. Degradation of organic contaminants in water with sulfate radicals generated by the conjunction of peroxymonosulfate with cobalt. *Environ. Sci. Technol.* **2003**, *37*, 4790–4797. [CrossRef]

7. Matta, R.; Tlili, S.; Chiron, S.; Barbati, S. Removal of carbamazepine from urban wastewater by sulfate radical oxidation. *Environ. Chem. Lett.* **2011**, *9*, 347–353. [CrossRef]

8. Hu, P.; Long, M. Cobalt-catalyzed sulfate radical-based advanced oxidation: A review on heterogeneous catalysts and applications. *Appl. Catal. B* **2016**, *181*, 103–117. [CrossRef]

9. Matzek, L.W.; Carter, K.E. Activated persulfate for organic chemical degradation: A review. *Chemosphere* **2016**, *151*, 178–188. [CrossRef]

10. Tsitonaki, A.; Petri, B.; Crimi, M.; Mosbæk, H.; Siegrist, R.L.; Bjerg, P.L. In situ chemical oxidation of contaminated soil and groundwater using persulfate: A review. *Crit. Rev. Environ. Sci. Technol.* **2010**, *40*, 55–91. [CrossRef]

11. Solís, R.R.; Rivas, F.J.; Tierno, M. Monopersulfate photocatalysis under 365 nm radiation. Direct oxidation and monopersulfate promoted photocatalysis of the herbicide tembotrione. *J. Environ. Manag.* **2016**, *181*, 385–394. [CrossRef]

12. Solís, R.R.; Rivas, F.J.; Chávez, A.M.; Dionysiou, D.D. Simulated solar photo-assisted decomposition of peroxymonosulfate. Radiation filtering and operational variables influence on the oxidation of aqueous bezafibrate. *Water Res.* **2019**, *162*, 383–393. [CrossRef]

13. Solís, R.R.; Rivas, F.J.; Gimeno, O. Removal of aqueous metazachlor, tembotrione, tritosulfuron and ethofumesate by heterogeneous monopersulfate decomposition on lanthanum-cobalt perovskites. *Appl. Catal. B* **2017**, *200*, 83–92. [CrossRef]

14. Tracking the Acute Toxicity of Sodium Sulfite. Available online: http://www.chemcas.com/material/cas/archive/7727-21-1.asp (accessed on 12 July 2019).

15. Tracking the Acute Toxicity of Potassium Peroxymonosulfate. Available online: http://datasheets.scbt.com/sc-253223.pdf (accessed on 12 July 2019).

16. Sra, K.S.; Thomson, N.R.; Barker, J.F. Stability of activated persulfate in the presence of aquifer solids. *Soil Sediment Contam.* **2014**, *23*, 820–837. [CrossRef]

17. Block, P.A.; Brown, R.A.; Robinson, D. Novel activation technologies for sodium persulfate in situ chemical oxidation. In Proceedings of the 4th International Conference on the remediation of chlorinated and recalcitrant compounds, Columbus, OH, USA, 24–27 May 2004.

18. Yen, C.H.; Chen, K.F.; Kao, C.M.; Liang, S.H.; Chen, T.Y. Application of persulfate to remediate petroleum hydrocarbon-contaminated soil: Feasibility and comparison with common oxidants. *J. Hazard. Mater.* **2011**, *186*, 2097–2102. [CrossRef]

19. Watts, R.J.; Teel, A.L. Treatment of contaminated soils and groundwater using ISCO. *Pract. Period. Hazard. Toxic Radioact. Waste Manag.* **2006**, *10*, 2–9. [CrossRef]

20. Liu, H.; Bruton, T.A.; Doyle, F.M.; Sedlak, D.L. In situ chemical oxidation of contaminated groundwater by persulfate: Decomposition by Fe (III)-and Mn (IV)-containing oxides and aquifer materials. *Environ. Sci. Technol.* **2014**, *48*, 10330–10336. [CrossRef]

21. Chen, L.; Peng, X.; Liu, J.; Li, J.; Wu, F. Decolorization of Orange II in aqueous solution by an Fe (II)/sulfite system: Replacement of persulfate. *Ind. Eng. Chem. Res.* **2012**, *51*, 13632–13638. [CrossRef]

22. Chen, L.; Tang, M.; Chen, C.; Chen, M.; Luo, K.; Xu, J.; Zhou, D.; Wu, F. Efficient bacterial inactivation by transition metal catalyzed auto-oxidation of sulfite. *Environ. Sci. Technol.* **2017**, *51*, 12663–12671. [CrossRef]

23. Chen, L.; Luo, T.; Yang, S.; Xu, J.; Liu, Z.; Wu, F. Efficient metoprolol degradation by heterogeneous copper ferrite/sulfite reaction. *Environ. Chem. Lett.* **2018**, *16*, 599–603. [CrossRef]

24. Zhou, D.; Chen, L.; Li, J.; Wu, F. Transition metal catalyzed sulfite auto-oxidation systems for oxidative decontamination in waters: A state-of-the-art minireview. *Chem. Eng. J.* **2018**, *346*, 726–738. [CrossRef]

25. Tracking the Acute Toxicity of Potassium Persulfate. Available online: http://www.chemcas.com/material/cas/archive/7757-83-7_v1.asp (accessed on 12 July 2019).

26. Reddy, K.B.; Van Eldik, R. Kinetics and mechanism of the sulfite-induced autoxidation of Fe(II) in acidic aqueous solution. *Atmos. Environ. Part A* **1992**, *26*, 661–665. [CrossRef]

27. Neta, P.; Huie, R.E. Free-radical chemistry of sulfite. *Environ. Health Perspect.* **1985**, *64*, 209–217. [CrossRef]

28. Alexander, B.; Park, R.J.; Jacob, D.J.; Gong, S. Transition metal-catalyzed oxidation of atmospheric sulfur: Global implications for the sulfur budget. *J. Geophys. Res. Atmos.* **2009**, *114*, D02309. [CrossRef]

29. Berglund, J.; Elding, L.I. Manganese-catalysed autoxidation of dissolved sulfur dioxide in the atmospheric aqueous phase. *Atmos. Environ.* **1995**, *29*, 1379–1391. [CrossRef]

30. Hui, P.K.; Palmer, H.J. Uncatalyzed oxidation of aqueous sodium sulfite and its ability to simulate bacterial respiration. *Biotechnol. Bioeng.* **1991**, *37*, 392–396. [CrossRef]

31. Fuller, E.C.; Crist, R.H. The rate of oxidation of sulfite ions by oxygen. *J. Am. Chem. Soc.* **1941**, *63*, 1644–1650. [CrossRef]

32. Sun, B.; Guan, X.; Fang, J.; Tratnyek, P.G. Activation of manganese oxidants with bisulfite for enhanced oxidation of organic contaminants: The involvement of Mn(III). *Environ. Sci. Technol.* **2015**, *49*, 12414–12421. [CrossRef]

33. Sun, B.; Dong, H.; He, D.; Rao, D.; Guan, X. Modeling the kinetics of contaminants oxidation and the generation of manganese (III) in the permanganate/bisulfite process. *Environ. Sci. Technol.* **2016**, *50*, 1473–1482. [CrossRef]

34. Sun, B.; Xiao, Z.; Dong, H.; Ma, S.; Wei, G.; Cao, T.; Guan, X. Bisulfite triggers fast oxidation of organic pollutants by colloidal MnO_2. *J. Hazard. Mater.* **2019**, *363*, 412–420. [CrossRef]

35. Lohner, S.T.; Tiehm, A. Application of electrolysis to stimulate microbial reductive PCE dechlorination and oxidative VC biodegradation. *Environ. Sci. Technol.* **2009**, *43*, 7098–7104. [CrossRef]

36. Yuan, S.; Chen, M.; Mao, X.; Alshawabkeh, A.N. A three-electrode column for Pd-catalytic oxidation of TCE in groundwater with automatic pH-regulation and resistance to reduced sulfur compound foiling. *Water Res.* **2013**, *47*, 269–278. [CrossRef]

37. Chen, L.; Xu, G.; Rui, Z.; Alshawabkeh, A.N. Demonstration of a feasible energy-water-environment nexus: Waste sulfur dioxide for water treatment. *Appl. Energy* **2019**, *250*, 1011–1022. [CrossRef]

38. Vandenberg, L.N.; Hauser, R.; Marcus, M.; Olea, N.; Welshons, W.V. Human exposure to bisphenol A (BPA). *Reprod. Toxicol.* **2007**, *24*, 139–177. [CrossRef]

39. Kang, J.H.; Aasi, D.; Katayama, Y. Bisphenol A in the aquatic environment and its endocrine-disruptive effects on aquatic organisms. *Crit. Rev. Toxicol.* **2007**, *37*, 607–625. [CrossRef]

40. Rao, D.; Sun, Y.; Shao, B.; Qiao, J.; Guan, X. Activation of oxygen with sulfite for enhanced Removal of Mn(II): The involvement of $SO_4^{\bullet-}$. *Water Res.* **2019**, *157*, 435–444. [CrossRef]

41. Soman, A.; Qiu, Y.; Chan Li, Q. HPLC-UV method development and validation for the determination of low level formaldehyde in a drug substance. *J. Chromatogr. Sci.* **2008**, *46*, 461–465. [CrossRef]

42. Lu, J.; Dreisinger, D.B.; Cooper, W.C. Anodic oxidation of sulphite ions on graphite anodes in alkaline solution. *J. Appl. Electrochem.* **1999**, *29*, 1161–1170. [CrossRef]

43. Available online: http://mmsphyschem.com/tblSRP.pdf (accessed on 10 July 2019).

44. Huie, R.E.; Neta, P. The chemical behavior of $SO_3^{\bullet-}$ and $SO_5^{\bullet-}$ radicals in aqueous solutions. *J. Phys. Chem.* **1984**, *88*, 5665–5669. [CrossRef]

45. Deister, U.; Warneck, P. Photooxidation of sulfite (SO_3^{2-}) in aqueous solution. *J. Phys. Chem.* **1990**, *94*, 2191–2198. [CrossRef]

46. Eibenberger, H.; Steenken, S.; O'Neill, P.; Schulte-Frohlinde, D. Pulse radiolysis and electron spin resonance studies concerning the reaction of SO4•− with alcohols and ethers in aqueous solution. *J. Phys. Chem.* **1978**, *82*, 749–750. [CrossRef]

47. Nguyen, T.B.; Doong, R.A.; Huang, C.P.; Chen, C.W.; Dong, C.D. Activation of persulfate by CoO nanoparticles loaded on 3D mesoporous carbon nitride (CoO@ meso-CN) for the degradation of methylene blue (MB). *Sci. Total Environ.* **2019**, *675*, 531–541. [CrossRef]

48. Li, R.; Kong, J.; Liu, H.; Chen, P.; Liu, G.; Li, F.; Lv, W. A sulfate radical based ferrous–peroxydisulfate oxidative system for indomethacin degradation in aqueous solutions. *RSC Adv.* **2017**, *7*, 22802–22809. [CrossRef]

49. Rickman, K.A.; Mezyk, S.P. Kinetics and mechanisms of sulfate radical oxidation of β-lactam antibiotics in water. *Chemosphere* **2010**, *81*, 359–365. [CrossRef]

50. Ghanbari, F.; Moradi, M.; Gohari, F. Degradation of 2, 4, 6-trichlorophenol in aqueous solutions using peroxymonosulfate/activated carbon/UV process via sulfate and hydroxyl radicals. *J. Water Proc. Eng.* **2016**, *9*, 22–28. [CrossRef]

51. Hayon, E.; Treinin, A.; Wilf, J. Electronic spectra, photochemistry, and autoxidation mechanism of the sulfite-bisulfite-pyrosulfite systems. SO_2^-, SO_3^-, SO_4^-, and SO_5^- radicals. *J. Am. Chem. Soc.* **1972**, *94*, 47–57. [CrossRef]

52. Buxton, G.V.; Greenstock, C.L.; Helman, W.P.; Ross, A.B. Critical review of rate constants for reactions of hydrated electrons, hydrogen atoms and hydroxyl radicals (·OH/·O−) in aqueous solution. *J. Phys. Chem. Ref. Data* **1988**, *17*, 513–886. [CrossRef]